第 36 卷 第 3 期
2019 年 9 月

原 子 核 物 理 评 论
Nuclear Physics Review

Vol. 36, No. 3
Sep. , 2019

文章编号： 1007-4627(2019) 03-0278-11

Effect of Strong Electric Field on the Evolution of Charmonium in Quark Gluon Plasma

WU Biaogang[1,2], CHEN Baoyi[3], ZHAO Xingbo[1,2,†]

(*1. Institute of Modern Physics, Chinese Academy of Sciences, Lanzhou 730000, China;*
2. School of Nuclear Science and Technology, University of Chinese Academy of Sciences, Beijing 100049, China;
3. Department of Physics, Tianjin University, Tianjin 300350, China)

Abstract: In ultra-relativistic heavy-ion collisions, the strong electric field can be produced by the colliding nuclei. The magnitude of the electric field E is on the order of $eE \sim m_\pi^2$ at the early stage of the collision. In quark gluon plasma (QGP), such a strong electric field can have a significant impact on the evolution of charmonia. We employ the time-dependent Schrödinger equation to study the evolution of charmonium states in the strong electric field generated by the moving charges. The electric field can result in transitions between charmonium states with different angular momenta. In order to see this effect, we make comparisons between the yields of J/ψ, ψ' and χ_c with and without the electric field. The results show that the electric field generated by the moving heavy ions induces dissociation of J/ψ. In the meantime, χ_c is generated via the transition from J/ψ by the electric field.

Key words: charmonium; strong electric field; QGP; Schrödinger equation

CLC number: O572.24+3; **Document code:** A **DOI:** 10.11804/NuclPhysRev.36.03.278

1 Introduction

Deconfined quark-gluon plasma (QGP) is expected to form in relativistic heavy-ion collisions due to high energy density and high temperature. Relativistic Heavy-Ion Collider (RHIC) at Brookhaven National Laboratory (BNL) performs experiments in Au-Au collisions at center-of-mass energy $\sqrt{s_{\rm NN}}$=200 GeV per nucleon pair. Large Hadron Collider (LHC) at CERN performs experiments in Pb-Pb collisions at center-of-mass energy $\sqrt{s_{\rm NN}}$=2.76 TeV. A lot of signals indicating the existence of QGP have been observed and studied in details in the past decades[1–6]. Heavy quarkonia, due to their large mass, have been proposed as one of the ideal probes for the early stages of heavy ion collisions[7]. Charmonium mass spectrum has been well studied with the parameterized Cornell potential, where relevant parameters can be fixed by the mass of low-lying charmonium states in vacuum[8–11]. At finite temperature, lattice QCD calculations suggest that the heavy quark potential inside quarkonium is partially screened by the deconfined medium[12]. Color screening effect sequentially melts the charmonium bound states at different temperatures.

The charmonium binding energy is usually taken as the difference between the charmonium mass and the open-charm threshold,

$$\epsilon_{\rm B}^0 = 2m_{\rm D} - m_\Psi, \tag{1}$$

with $m_{\rm D} \simeq$1.87 GeV. In vacuum the $D\bar{D}$ pair is usually considered as the open charm threshold for charmonium states. The low-lying charmonium states typically have binding energies on the order of several hundred MeV, *e.g.*, $\epsilon_{\rm B}^{J/\psi}$=640 MeV.

In relativistic heavy-ion collisions, external electric field is produced by colliding heavy ions and is on the order of a few m_π^2 in the early stage of the collisions[13]. Note that J/ψ mean radius is around $\langle r\rangle_{J/\psi} \sim$0.5 fm. The electric potential energy between c and $\bar{c}$, $eE\langle r\rangle$, is about several hundred MeV which is comparable with the binding energy of charmonium states. Therefore, it is necessary to study the effects of external electric field on the evolution of charmonium

---

Received date: 25 Mar. 2019; **Revised date:** 5 May 2019

Foundation item: National Natural Science Foundation of China(11705125); New faculty startup funding by Institute of Modern Physics, Chinese Academy of Sciences

Biography: WU Biaogang(1989–), male, Xinxiang, Henan Province, Graduate student, working on heavy-ion collision physics; E-mail: wubg@impcas.ac.cn

† **Corresponding author:** ZHAO Xingbo, E-mail: xbzhao@impcas.ac.cn.

states in the deconfined medium. In this work, we focus on the effects of initial electric field on primordially produced charmonium.

The paper is organized as follows. In Sec. 2, a brief introduction to the method we used in our calculation is presented. We explain the origin of screening effect of QGP and the source of the time-dependent electric field in the collision. In the end of this section we give the angular-momentum decomposed form of the Hamiltonian. Sec. 3 shows numerical results with both electric field and QGP and a comparison is made with the results without electric field. Finally, conclusions and outlook are given in Sec. 4.

2 Framework

We adopt the non-relativistic Schrödinger equation to describe the evolution of the charmonium states in QGP[14],

$$\mathrm{i}\frac{\partial}{\partial t}\psi(r,\theta)=\hat{H}\psi(r,\theta),$$
$$\hat{H}=\frac{1}{2\mu}\hat{p}^2+V_{\bar{\mathrm{q}}\mathrm{q}}(r;T)+V_E(r,\theta), \tag{2}$$

here $r=|\boldsymbol{r}_c-\boldsymbol{r}_{\bar{c}}|$ is the length of the relative coordinate between c and $\bar{c}$. $\psi(r,\theta)$ is the wave function of the charmonium and μ is the reduced mass. We take charm quark mass as 1.25 GeV in our calculation. $V_{\bar{\mathrm{q}}\mathrm{q}}(r;T)$ is the potential between c and $\bar{c}$ and it depends on the temperature T of the medium after heavy-ion collisions. $V_E(r,\theta)$ is the potential of the electric field. We will give detailed explanations of these two potentials in the following parts.

2.1 The potential between c and $\bar{c}$ in QGP

Heavy quarks move inside the charmonium with a speed $\langle v^2/c^2\rangle$ ~0.25 for J/ψ[14]. The charmonium can be described in non-relativistic Schrödinger approach with the Cornell potential which gives the mass spectrum of the charmonium states[8–9],

$$V_{\bar{\mathrm{q}}\mathrm{q}}(r;T=0)=-\frac{4}{3}\frac{\alpha_s}{r}+\sigma r, \tag{3}$$

with $\alpha_s\simeq0.2$ and $\sigma\simeq1$ GeV/fm[15]. The first term originates from the one-gluon exchange interaction, and the second linear term reflects the confining interaction.

If a charmonium is immersed in QGP, the color force between c and $\bar{c}$ is screened by the surrounding colored partons in a way similar to the electron plasma: the $c(\bar{c})$ quark attracts partons with opposite color charges and forms the “Debye cloud”. A phenomenological ansatz for the screened Cornell potential[16] is,

$$V_{\bar{\mathrm{q}}\mathrm{q}}(r;T)=\frac{\sigma}{\mu_{\mathrm{D}}(T)}\left(1-\mathrm{e}^{-\mu_{\mathrm{D}}(T)r}\right)-\frac{4\alpha_s}{3r}\mathrm{e}^{-\mu_{\mathrm{D}}(T)r}. \tag{4}$$

Debye-screening lowers the charmonium binding energies, and contributes to the charmonium dissociation rate. According to thermal pQCD, the Debye mass is related to the temperature of the medium T via

$$\mu_{\mathrm{D}}^2(T)=g^2T^2\left(\frac{N_{\mathrm{c}}}{3}+\frac{N_{\mathrm{f}}}{6}\right), \tag{5}$$

here g=1.5 is the strong coupling constant. $N_{\mathrm{c}}=3$ is the number of colors and N_{f}=3 is the number of flavors. The vacuum Cornell potential and the screened Cornell potentials at different temperatures are shown in Fig. 1(a). We can see that the screened Cornell potential at large r decreases with temperature. The confining potential becomes very weak at temperature above critical temperature T_{c}=170 MeV[17]. From Fig. 1, at sufficiently high temperature c and $\bar{c}$ cannot form bound state any more because the color interaction between them is screened. Based on this mechanism J/ψ suppression was first suggested in 1986 as a signature of QGP[7]. In this paper we ignore the spin degrees of freedom and thus the fine splittings are ignored. $J/\psi,\psi'$, and χ_{c} denote the eigenstates of the vacuum Cornell potential in Eq. (3) and throughout this paper they are used interchangeably with 1S, 2S,

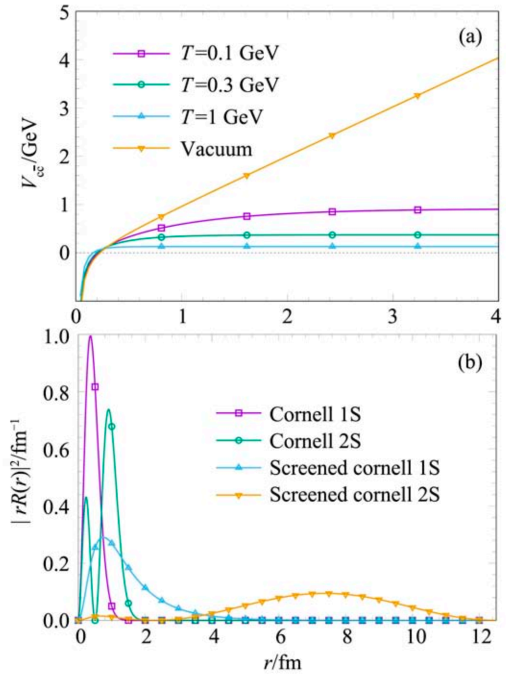

Fig. 1 (color online) Radial profile of Cornell potential and resulting charmonium wave functions in vacuum and at finite temperatures. (a) The vacuum Cornell potential and the screened Cornell potential at different temperatures; (b) Radial distribution of the 1S and 2S state of the vacuum Cornell potential and the screened Cornell potential.

and 1P, respectively. 1S and 2S eigenstates of the vacuum Cornell potential and the screened Cornell potential are compared in Fig. 1(b). We see that the eigenstates of the screened Cornell potential tend to dissolve.

2.2 Electric field in QGP after heavy-ion collisions

Ultra-relativistic heavy-ion collisions can create a strong and time-dependent electric field with a peak magnitude $eE \sim m_\pi^2$[18]. The electric field $E(t)$ in this work originates from two moving heavy ions with impact parameter b and is schematically shown in Fig. 2.

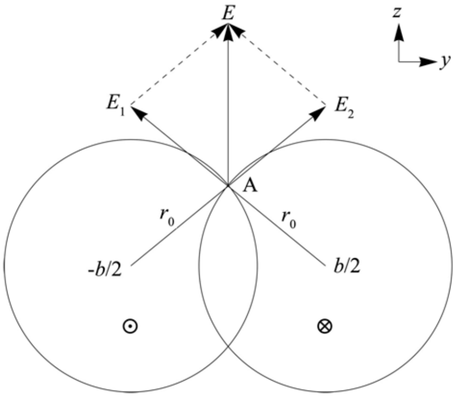

Fig. 2 Schematic geometry in the transverse plane of the two moving heavy ions. The electric field at point A is a combination of the electric fields generated by the two moving heavy ions.

Electric field generated by moving charges after heavy ion collisions is position-dependent. In order to see the magnitude of the effect of the electric field on the evolution of the charmonium states, we take a representative point A located at the surface of the intersection of the two heavy ions as shown in Fig. 2. The heavy ions are moving in the direction perpendicular to the plane of the page and the heavy ion on the right side is moving inward while the other one is moving outward. The electric field at point A generated by the two moving heavy-ions is given by Eq. (7). It is in z direction and is the combination of the electric fields generated by the two moving heavy ions. In our calculation the electric field is taken as a uniform electric field identical to the electric field at point A. We defer the study of non-uniform electric field to a future paper. Because the electric field strength at point A is the maximum in the intersection of the two heavy ions, our calculation provides an estimation of the maximum effect of the electric field generated during the collisions. The electric field strength at point A generated by one of the two moving heavy ions with a radius r_0 and Lorentz factor $\gamma = \frac{1}{\sqrt{1-v^2}}$ is[19]:

$$E = \frac{\gamma Z e r_0}{(r_0^2 + \gamma^2 v^2 t^2)^{3/2}}, \tag{6}$$

which gives the total electric field strength at point A as:

$$\begin{aligned} eE &= \frac{\gamma Z e^2 r_0}{(r_0^2 + \gamma^2 v^2 t^2)^{3/2}} \cdot \frac{2\sqrt{r_0^2 - \left(\frac{b}{2}\right)^2}}{r_0} \\ &= \frac{4\pi\alpha\gamma Z\sqrt{4r_0^2 - b^2}}{\left(r_0^2 + \gamma^2 v^2 t^2\right)^{3/2}}, \end{aligned} \tag{7}$$

here $\alpha = \frac{1}{137}$ is the electromagnetic coupling constant. Z is the proton number. A is the relative atomic mass and r_0 is the radius of heavy ions[20]:

$$r_0 = 1.1 A^{\frac{1}{3}}(\mathrm{fm}). \tag{8}$$

Considering the nuclear transparency in high energy heavy-ion collisions[21–22], we approximate that the heavy ions move in a constant velocity for simplicity. Fig. 3 shows the time-dependence of the $eE(\gamma, t)$ generated by two gold nuclei with impact parameter b=10 fm at different γ's. t=0 is defined as the moment of the collision.

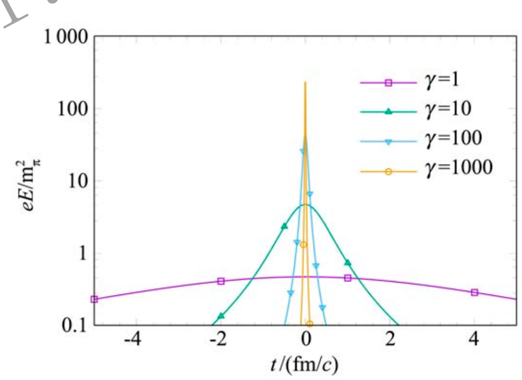

Fig. 3 (color online) Time profile of the electric field, $eE(\gamma, t)$, generated by colliding heavy ions in the unit of m_π^2 (with m_π^2=0.018 GeV^2).

As shown in Fig. 3 the electric field vanishes quickly after the collision. We define the lifetime of the electric field as the time it takes for the electric field to decrease from its peak value to 10% of the peak value. The peak magnitude of eE increases with γ, while the electric field's lifetime decreases rapidly with γ. Notice that the charm pair is produced at almost the same point and evolves into a certain charmonium state with a time scale ~0.5 fm/c[23]. During the short lifetime of the electric fields, the charm pair is in a superposition of the eigenstates of the Cornell potential. In this work, as an approximation we assume that the charm pairs evolve into the charmonium states instantly, and neglect the formation process and the interaction with the medium in the meantime. On the other hand, the medium's none-zero electrical conductivity may have an impact on the duration of the electric field[24]: the time-varying electric field of the moving heavy ions induces eddy currents which in turn magnify the magnitude of the electric field and prolong its lifetime. In this paper we conduct a scholastic research on the effects of strong electric fields in charmonium production. We defer the study of the medium effect to a future work.

2.3 Hamiltonian

The wave function of the charmonium states can be represented as:

$$\psi(r,\theta,\phi)=\sum_{lm}R_{lm}(r)Y_l^m(\theta,\phi), \tag{9}$$

where $Y_l^m(\theta,\phi)$ are spherical harmonics. In this case, considering that the electric field does not change the magnetic quantum number m, we choose the states in our calculation with m=0. We consider the charmonium states with mass up to 4 GeV (in vacuum) which include specifically 1S (J/ψ), 2S (ψ'), 1P (χ_c), 2P and 1D. Their respective masses from Eq. (3) are $m_{J/\psi}$=3.09 GeV, $m_{\psi'}$=3.70 GeV, m_{χ_c}=3.48 GeV, m_2P=3.98 GeV and m_1D=3.78 GeV.

For the radial wave function, we define $U(r)=rR(r)$. The radial Hamiltonian in Eq. (2) can then be written as:

$$\mathcal{H}=-\frac{1}{2\mu}\frac{\partial^2}{\partial r^2}+V_{\bar{\text{q}}\text{q}}(r)+\frac{l\,(l+1)}{2\mu r^2}-Er\cos\theta. \tag{10}$$

By multiplying each side of the Schrödinger equation by $\sum_l |Y_l^0(\theta)\rangle\langle Y_l^0(\theta)|$ and integrating θ out we obtain the radial Schrödinger equation as:

$$\text{i}\frac{\partial}{\partial t}U_l(r)=\int \text{d}r'\sum_{l'}\mathcal{H}_{ll'}(r,r')U_{l'}(r'), \tag{11}$$

here $l=0,1,2,\cdots$ are the eigenvalues of angular momentum of the charmonium states and $U_l(r)$ is the radial wave function of the state with angular momentum l. Then the Hamiltonian $\mathcal{H}_{ll'}(r,r')$ in basis of spherical harmonics takes the following form:

$$\begin{aligned}
\mathcal{H}_0(r)&=-\frac{1}{2\mu}\frac{\partial^2}{\partial r^2}+V_{\bar{\text{q}}\text{q}}(r),\\
\mathcal{H}_{00}(r)&=\mathcal{H}_0(r),\\
\mathcal{H}_{01}(r)&=\mathcal{H}_{10}(r)=-\frac{\sqrt{3}}{3}Er,\\
\mathcal{H}_{11}(r)&=\mathcal{H}_0(r)+\frac{2}{2\mu r^2},\\
\mathcal{H}_{20}(r)&=\mathcal{H}_{02}(r)=0,\\
\mathcal{H}_{12}(r)&=-\frac{\sqrt{15}}{30}Er,\\
\mathcal{H}_{22}(r)&=\mathcal{H}_0(r)+\frac{6}{2\mu r^2}.
\end{aligned} \tag{12}$$

We use natural units $\hbar=c$=1. From the Hamiltonian we can see that the uniform electric field can only induce transitions between states that differ in angular momentum by 1, which is consistent with the selection rule for electric dipole transitions.

3 Numerical results

In solving the time-dependent Schrödinger equation, we use the MSD2 method[25]. In order to see the evolution of J/ψ, we make contour plots of $|\psi(r,\theta,\phi)|^2=\sum_l|R_l(r)|^2|Y_l^0(\theta,\phi)|^2$ at azimuthal angle ϕ=0 and $\phi=\pi$ (y-z plane) by taking into account the azimuthal symmetry. In the following sections we will compare with the evolution of radial distribution of $c(\bar{c})$ with and without the external electric field. Since at RHIC or LHC energy, the lifetime of the electric field is within 0.2 fm/c, and the lifetime of QGP is typically several fm/c, in this work we consider the evolution in the first 2 fm/c when the electric field and QGP have strongest impact on the production of charmonia.

3.1 Time evolution of J/ψ and χ_c in QGP at constant temperature without electric field

In this section we consider the charmonium states dissociation process at the constant temperature of 1.5 T_c, a typical temperature of QGP generated in heavy-ion collisions. Fig. 4 shows the dissociation process of J/ψ. The fractions are defined as the possibility of charmonium states projected onto the eigenstates of the vacuum Cornell potential.

In Fig. 4, the wave function of charmonium broadens with time which suggests that J/ψ is being dissociated by the colored partons in QGP. The fractions in Fig. 4(b) show the dissociation effect and the contour plots show that the evolved wave function of charmonium is still with spherical symmetry.

In Fig. 5 the initial state is taken to be χ_c, a P-wave state of the vacuum Cornell potential.

Since the Hamiltonian without electric field is spherically symmetric, the transitions between states with different angular momenta are forbidden. Comparing with Figs. 4 and 5, we see that χ_c is dissociated faster than J/ψ.

3.2 Time evolution of J/ψ and χ_c in QGP at decreasing temperature without electric field

As QGP expands after the collision, the temperature of the hot medium decreases. For simplicity we model the evolution of temperature as a linearly decreasing process in which temperature decreases from 1.5 T_c to T_c in 2 fm/c. Fig. 6 shows the evolution of

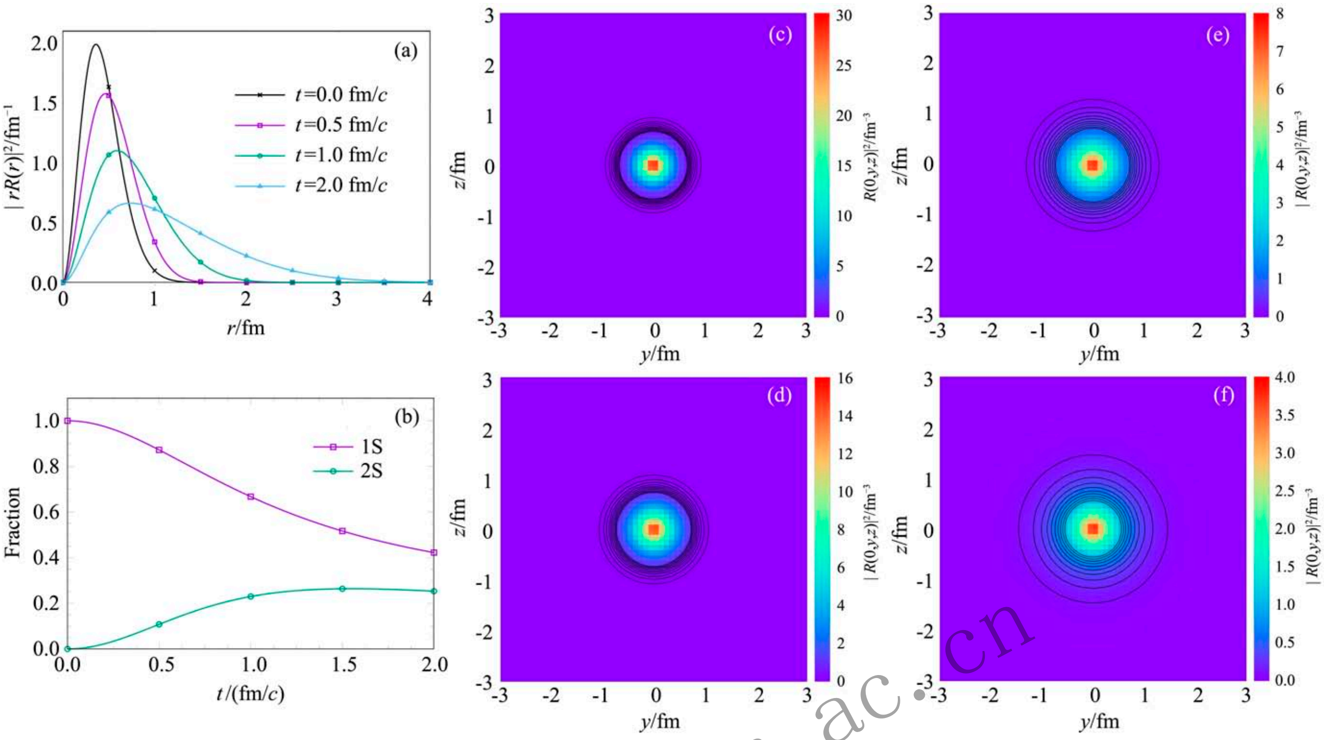

Fig. 4 (color online) Time dependence of the charmonium system in QGP at constant temperature without electric field. The initial state is J/ψ (in vacuum) and T=1.5 $T_{\rm c}$. The radial distribution $|rR(r,t)|^2$ of J/ψ is plotted in panel (a). The fractions are plotted in panel (b). The radial distribution of $c(\bar{c})$ at different time steps is plotted at (c) t=0 (d) t=0.5 fm/c, e) t=1 fm/c, f) t=2 fm/c.

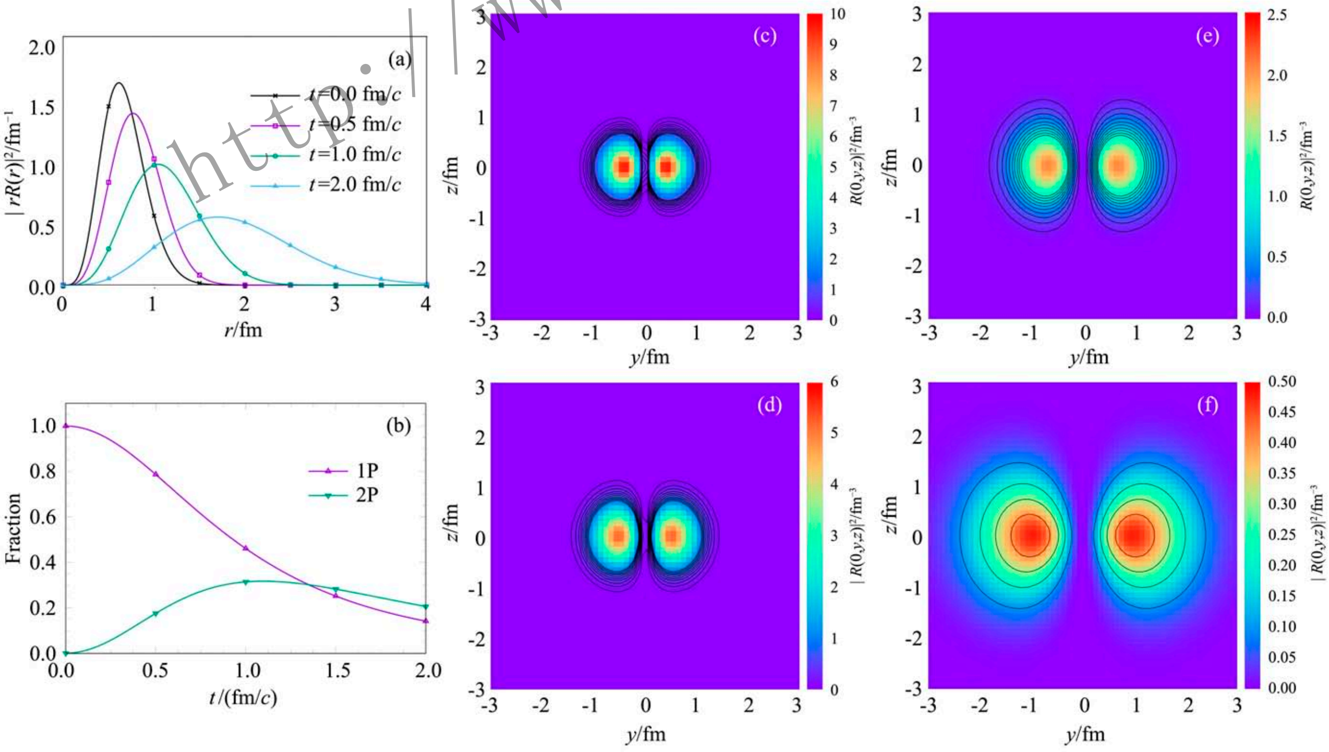

Fig. 5 (color online) Same as Fig. 4. The initial state is $\chi_{\rm c}$ (in vacuum) and T=1.5 $T_{\rm c}$. The radial distribution $|rR(r,t)|^2$ of $\chi_{\rm c}$ is plotted in panel (a). The fractions are plotted in panel (b). The radial distribution of $c(\bar{c})$ at different time steps is shown in (c) t=0, (d) t=0.5 fm/c, (e) t=1 fm/c, (f) t=2 fm/c.

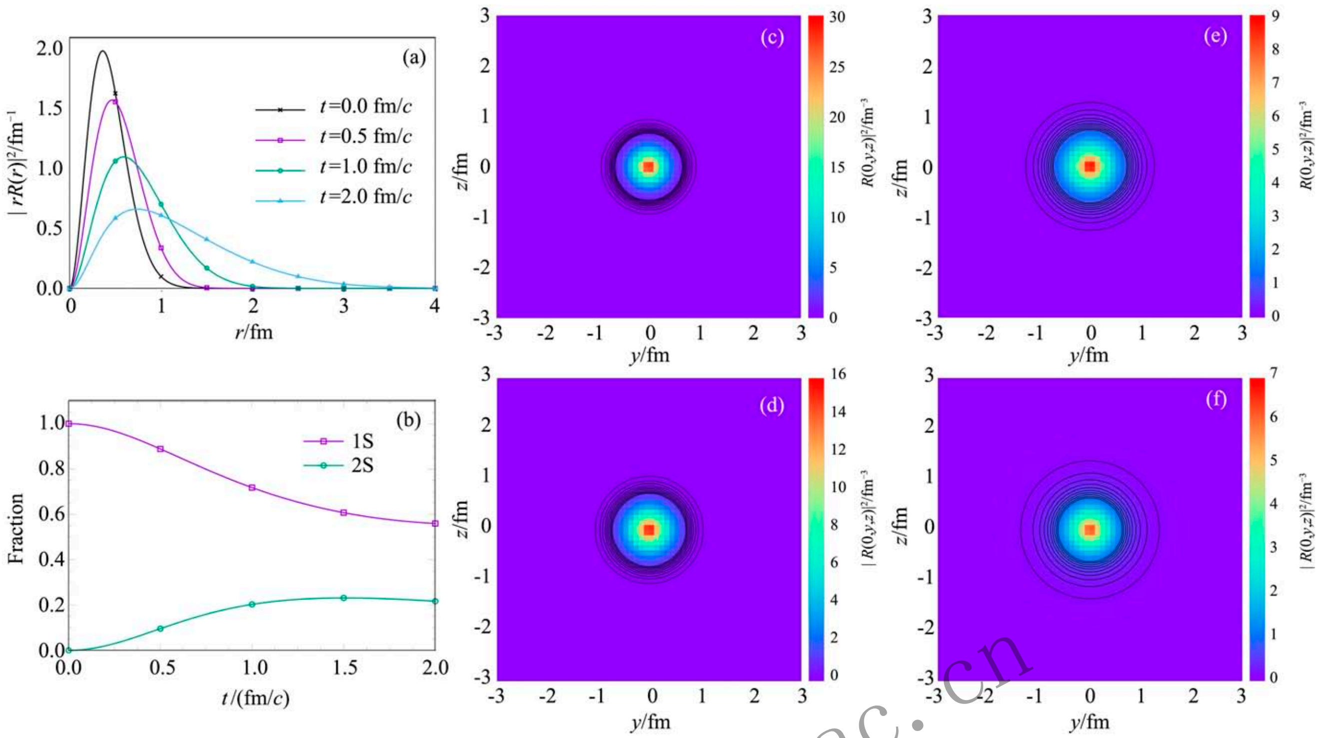

Fig. 6 (color online) Time dependence of the charmonium system in QGP at decreasing temperature without electric field. The initial state is J/ψ (in vacuum). And the temperature in the screened Cornell potential decreases linearly in time from 1.5 T_c to T_c in 2 fm/c. The radial distribution $|rR(r,t)|^2$ of J/ψ is plotted in panel (a). The fractions are plotted in panel (b). The radial distribution of $c(\bar{c})$ at different time steps is shown in (c) t=0, d) t=0.5 fm/c, (e) t=1 fm/c, (f) t=2 fm/c.

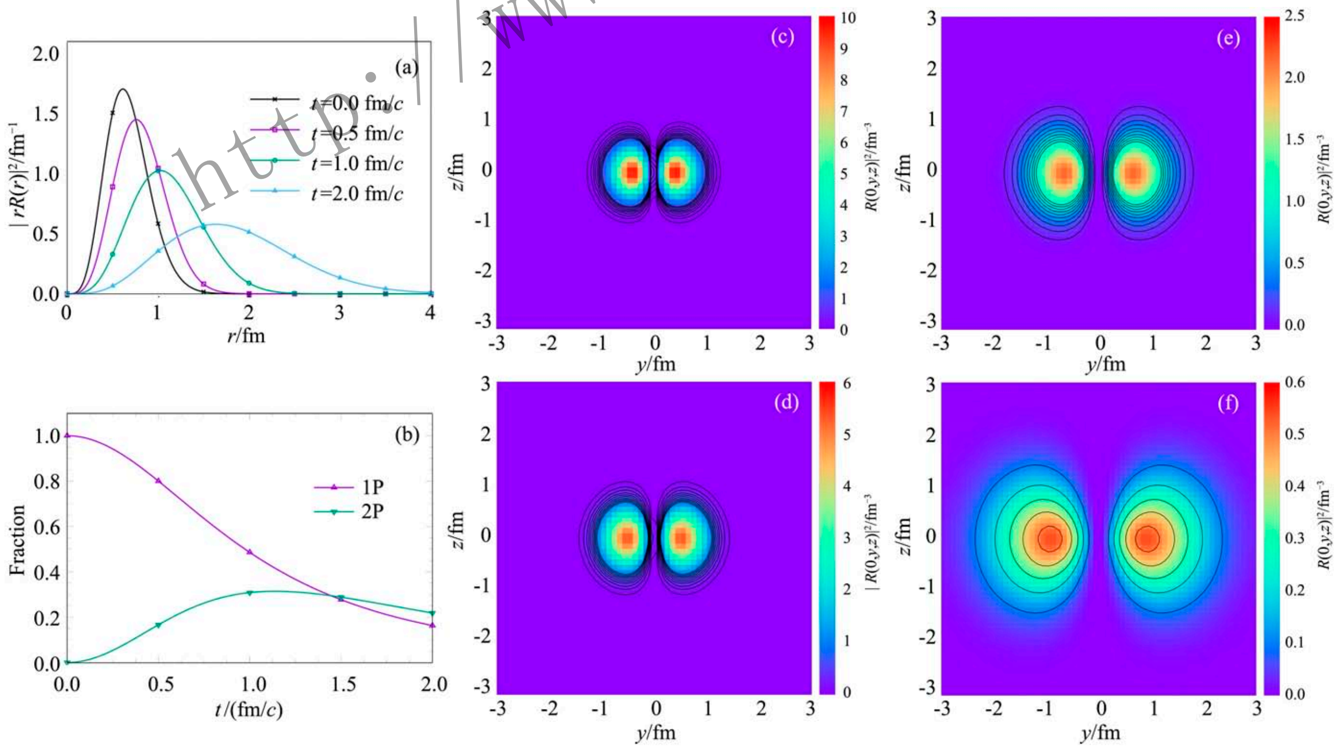

Fig. 7 (color online) Same as Fig. 6. The initial state is χ_c (in vacuum). The temperature in the screened Cornell potential decreases linearly from 1.5 T_c to T_c uniformly in 2 fm/c. The radial part $|rR(r,t)|^2$ of χ_c is plotted in panel (a). The fractions are plotted in panel (b). The radial distribution of $c(\bar{c})$ at different time steps is shown in (c) t=0, (d) t=0.5 fm/c, (e) t=1 fm/c, (f) t=2 fm/c.

J/ψ in the cooling system. Comparing with Fig. 4b), we see that the rate of dissociation is slower than that at the constant temperature of 1.5 $T_{\rm c}$.

Fig. 7 shows the dissociation process of $\chi_{\rm c}$ in QGP with decreasing temperature. We can see that time-dependent temperature has a greater impact on the fractions of S wave states than those of P-wave states.

3.3 Time evolution of J/ψ and $\chi_{\rm c}$ in QGP at decreasing temperature with electric field

In the following parts we present the evolution of charmonium states in the electric field introduced in Sec. 2.2. Meanwhile the temperature is assumed to drop linearly in time from 1.5 $T_{\rm c}$ to $T_{\rm c}$ in 2 fm/c in this process.

3.3.1 Au-Au collision with $\gamma\simeq 100$

We first consider Au-Au collisions in RHIC with center-of-mass energy $\sqrt{s_{\rm NN}}$=200 GeV per nucleon pair with $\gamma\simeq$100. The lifetime of electric field is about 0.2 fm/c as shown in Fig. 3.

Fig. 8 shows the evolution of the charmonium system. For simplicity, the initial state is assumed to be J/ψ (in vacuum). The system is with both cooling QGP and the time-dependent electric field.

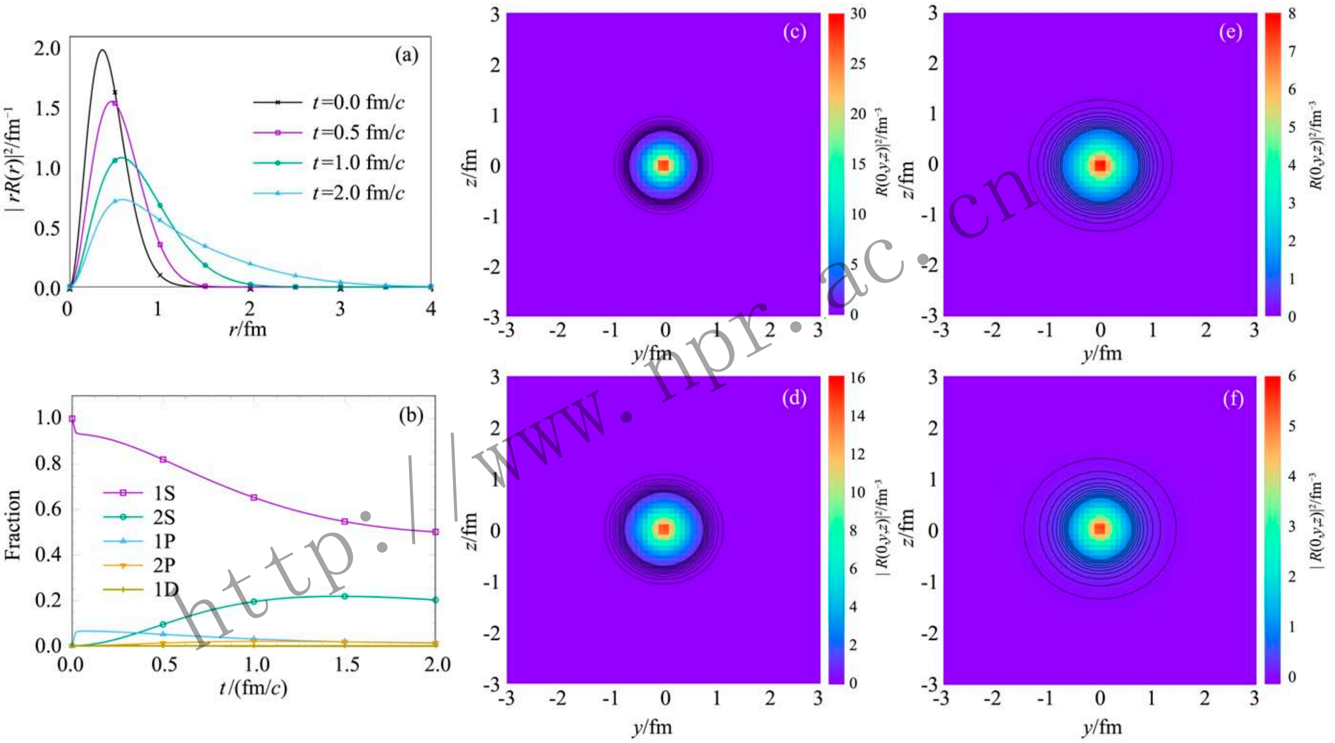

Fig. 8 (color online) Time dependence of the charmonium system in QGP at decreasing temperature with electric field in Au-Au collisions. The initial state is J/ψ (in vacuum). The radial distribution $|rR(r,t)|^2$ of J/ψ is plotted in panel (a). The fractions are plotted in panel (b). The radial distribution of $c(\bar{c})$ at different time steps is shown in (c) t=0, (d) t=0.5 fm/c, (e) t=1 fm/c, (f) t=2 fm/c.

As shown in Fig. 8, The fraction of J/ψ drops to 0.5 in 2 fm/c which is faster than the case without the electric field, see Fig. 6(b). In particular, the 1S fraction in Fig. 8(b) drops rapidly in the first 0.2 fm/c (∼the lifetime of the electric field at $\gamma\simeq$100). We note that the transition from 1S to 2S induced by the electric field is suppressed due to the selection rules for the electric dipole transitions. We also note that $\chi_{\rm c}$ is generated due to the strong electric field. As a result the radial distribution of $c(\bar{c})$ deviates from spherical symmetry.

In Fig. 9, the initial state of the charmonium is taken to be $\chi_{\rm c}$ (in vacuum).

Comparing to the case without the electric field (see Fig. 7), electric field induces transitions from 1P to 1S and 2S states. The fractions of the S-wave states and D-wave states are non-zero at t=2 fm/c, which are from the transitions of the $\chi_{\rm c}$ state. The contour plots indicate the S-wave components in the wave function because only S-wave states have non-zero probability at the origin. We note that the 1D state is slightly produced in the first 1 fm/c and is dissociated subsequently.

3.3.2 Pb-Pb collision with $\gamma\simeq 1000$

Now we consider Pb-Pb collisions in LHC with center-of-mass energy $\sqrt{s_{\rm NN}}$=2.76 TeV per nucleon pair. In our calculation we take γ=1 000 for simplicity. The lifetime of electric field is only about 0.1 fm/c as

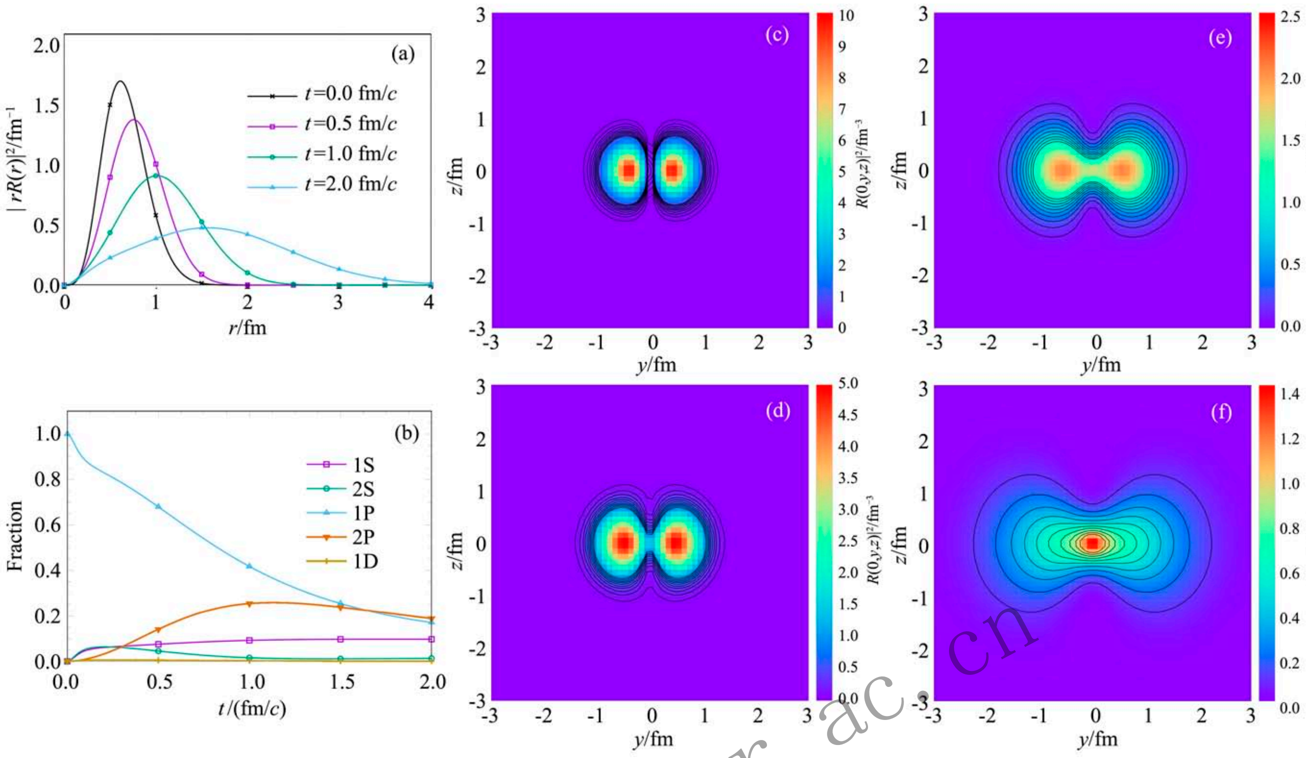

Fig. 9 (color online) Time dependence of the charmonium system in QGP at decreasing temperature with electric field in Au-Au collisions. The initial state is χ_c (in vacuum). The radial distribution $|rR(r,t)|^2$ of χ_c is plotted in panel (a). The fractions are plotted in panel (b). The radial distribution of $c(\bar{c})$ at different time steps is shown in (c) t=0, (d) t=0.5 fm/c, (e) t=1 fm/c, (f) t=2 fm/c.

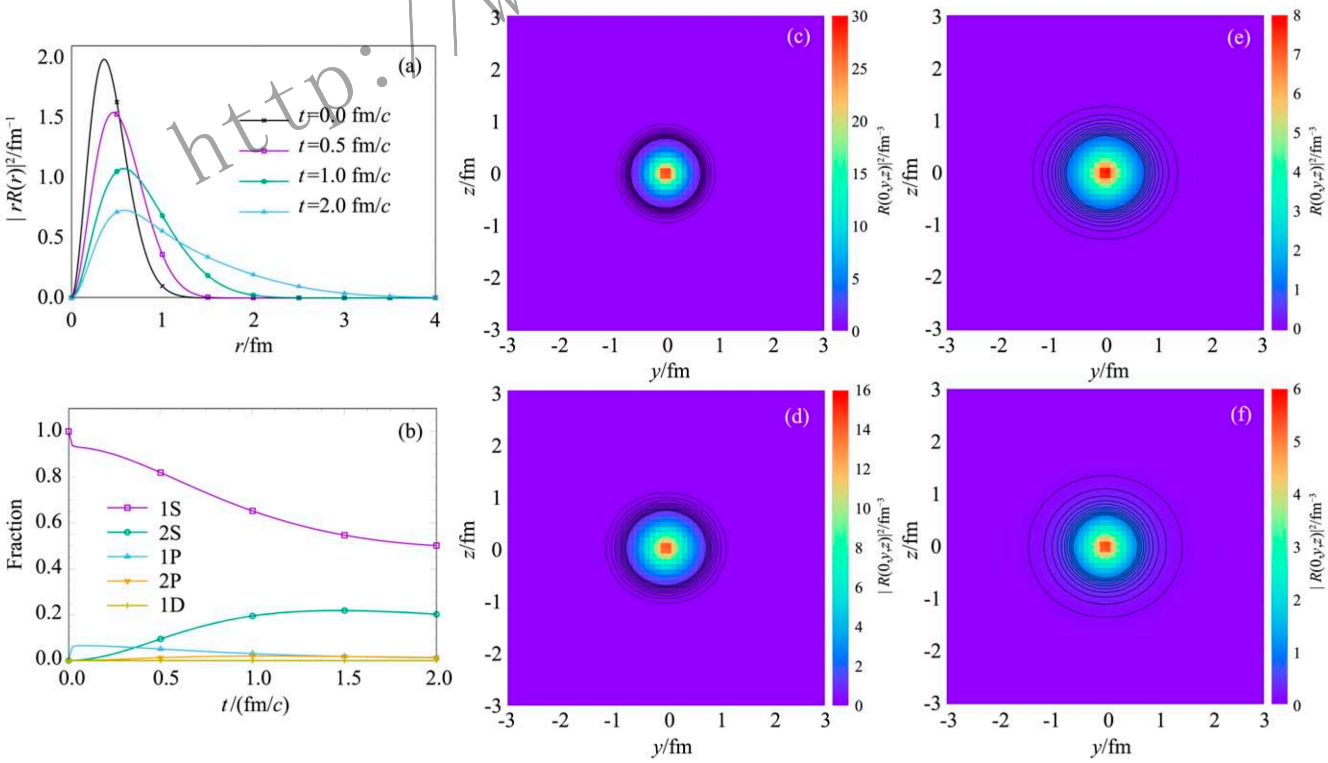

Fig. 10 (color online) Time dependence of the charmonium system in QGP at decreasing temperature with electric field in Pb-Pb collisions. The initial state is J/ψ (in vacuum). The radial distribution $|rR(r,t)|^2$ of J/ψ is plotted in panel (a). The fractions are plotted in panel (b). The radial distribution of $c(\bar{c})$ at different time steps is shown in (c) t=0, (d) t=0.5 fm/c, (e) t=1 fm/c, (f) t=2 fm/c.

shown in Fig. 3.

Fig. 10 shows the evolution of the charmonium system from the initial state of J/ψ (in vacuum). The system is with both cooling QGP and the time-dependent electric field.

In Fig. 10(b), in the first 0.02 fm/c, the strong electric field causes a significant drop in the fraction of 1S state and a rapid increase in the fraction of 1P state. The duration in which 1S fraction drops fastest is approximately the lifetime of the electric field at γ=1 000 as shown in Fig. 3. And the contour plots show that the radial distribution of $c(\bar{c})$ deforms from spherical symmetry significantly due to the strong electric field.

Fig. 11 shows the evolution of χ_c in the screened Cornell potential with decreasing temperature and the electric field generated in heavy-ion collisions with $\gamma\simeq$1 000.

Again, in the first 0.01 fm/c, the electric field causes a significant drop in the fraction of 1P state and correspondingly a rapid increase in the fractions of 1S and 2S state. This is different from Fig. 10(b) where only 1P state is generated rapidly.

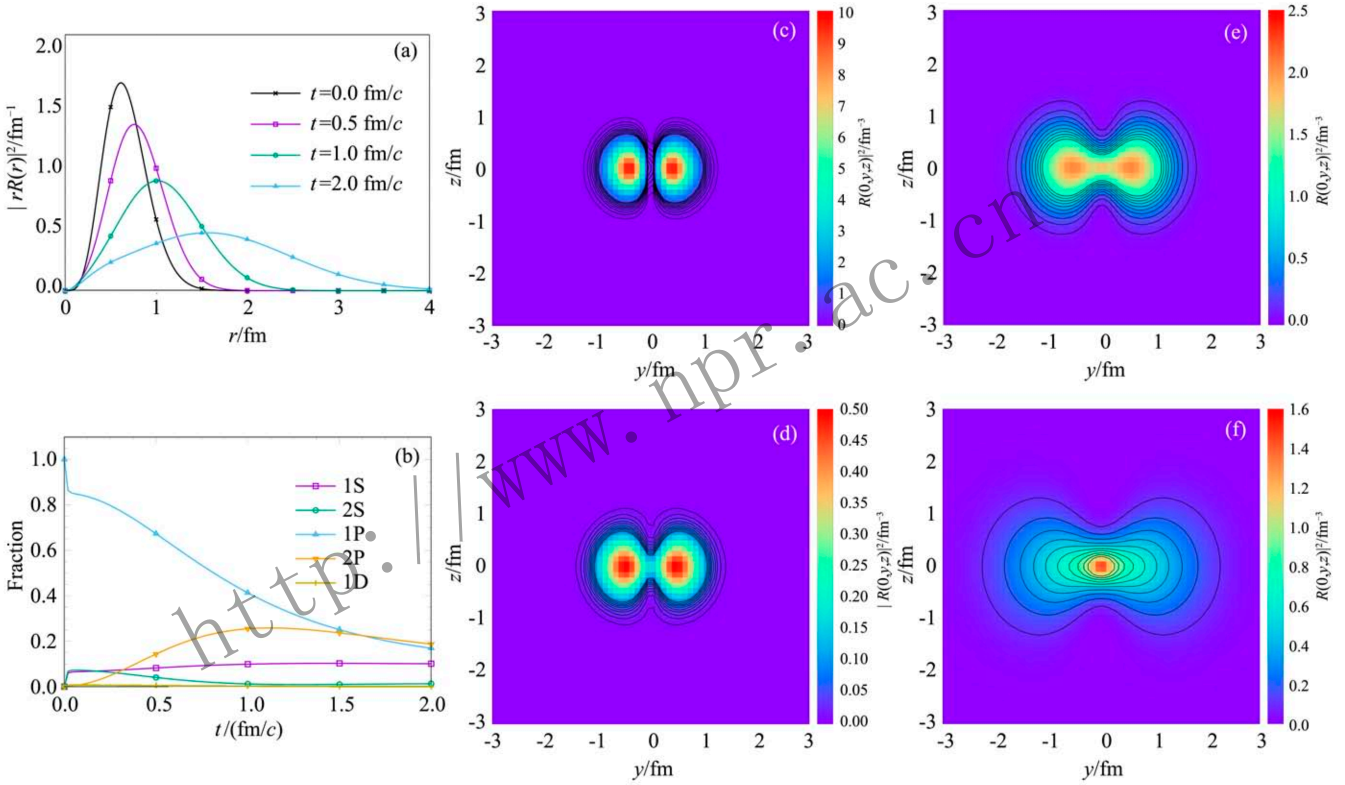

Fig. 11 (color online) Time dependence of the charmonium system in QGP at decreasing temperature with electric field in Pb-Pb collisions. The initial state is χ_c (in vacuum). The radial distribution $|rR(r,t)|^2$ of χ_c is plotted in panel (a). The fractions are plotted in panel (b). The radial distribution of $c(\bar{c})$ at different time steps is shown in (c) t=0, (d) t=0.5 fm/c, (e) t=1 fm/c, (f) t=2 fm/c.

3.3.3 Cu-Au collision with $\gamma \simeq 100$ and $\gamma \simeq$ 1 000

In this section we consider an asymmetric collision: the Cu-Au collision. The geometry of the colliding heavy ions is shown in Fig. 12.

As the same with the symmetric case, the electric field generated by Au and Cu ions is shown in Fig. 12 and is given by Eq. (13). Here a_1=1 fm is the distance between A (the center of the intersecting circle of the two ions) and the center of the Cu ion and a_2=4.9 fm is the distance between A and the center of the Au ion. Z_1 and Z_2 are the proton numbers of the Cu and Au ion respectively, and r_1 and r_2 are the radii of the Cu and Au ion respectively from Eq. (8). We can see that the magnitude of the electric field at A,

$$eE=\frac{4\pi\alpha\gamma Z_1 a_1^4}{(a_1^2+\gamma^2v^2t^2)^{3/2}r_1^3}-\frac{4\pi\alpha\gamma Z_2 a_2^4}{(a_2^2+\gamma^2v^2t^2)^{3/2}r_2^3}, \quad (13)$$

is smaller than that in Fig. 2.

For simplicity, we take the same temperature evolution profile as in Au-Au collisions. Fig. 13 shows the evolution of J/ψ and χ_c in the electric field generated in Cu-Au collisions with γ=100 and γ=1 000.

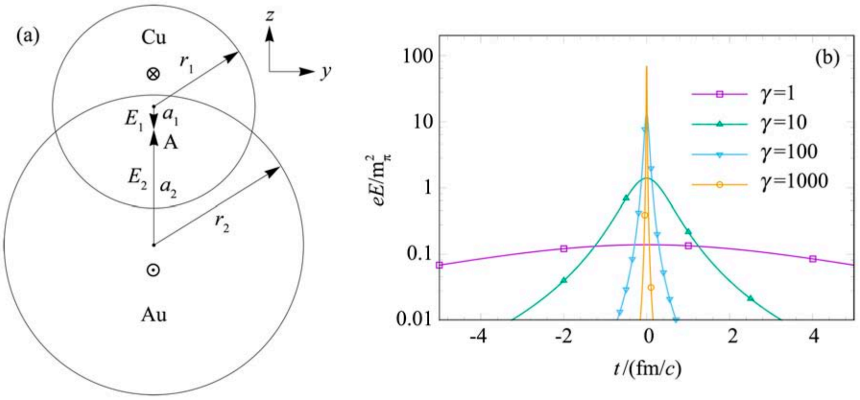

Fig. 12　Transverse geometry and time profile of the electric field created in Cu-Au collisions. (a) The electric field at point A is a combination of the electric fields generated by the moving Au and Cu ions. (b) $eE(\gamma,t)$ in the unit of m_π^2 (with m_π^2=0.018 GeV^2).

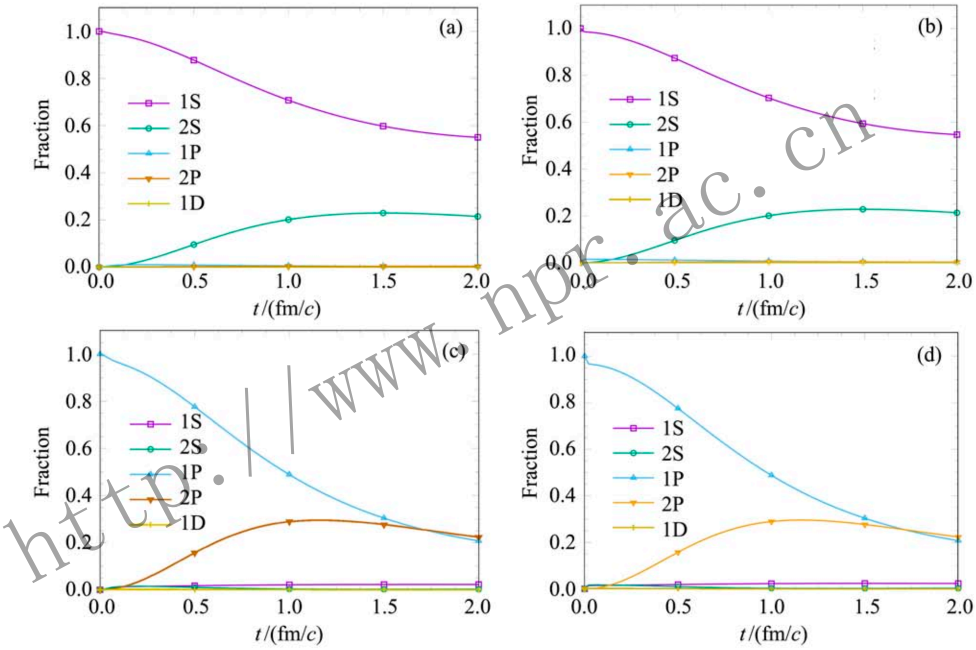

Fig. 13　(color online) Time evolution of the fractions of the charmonium states in Cu-Au collisions. The fractions from initial states of J/ψ (in vacuum) are plotted in (a) and (b). The fractions from initial states of $\chi_{\rm c}$ (in vacuum) are plotted in (c) and (d). In panel (a) and (c), γ=100, and in panel (b) and (d), γ=1 000.

4　Conclusions and outlook

In relativistic heavy-ion collisions, extremely hot medium can be produced which is expected to be the deconfined phase of nuclear matter. Besides, strong electric field is produced when two nuclei collide with each other at nearly the speed of light. We study the dissociation and transitions between different charmonium states caused by the electric field as well as the hot medium in Schrödinger equation formalism.

The electric field with large magnitude generates visible effects in the charmonium production in the early stage of the collisions. The charmonium states are dissociated more strongly than the case without electric field. Due to the selection rule for electric dipole transitions, the electric field converts some J/ψ to $\chi_{\rm c}$ states and vice versa.

In the future we plan to extend our study to a realistic non-uniform electric field. We will also adopt the more realistic initial states from pQCD calculations and a realistic temperature evolution profile. The effect of strong magnetic field created in relativistic heavy-ion collisions will be considered in our future work as well. In a similar way, this approach can be also used to study the evolution of bottomonia in QGP.

Acknowledgments: We thank DU Xiaojian for his codes. This work is supported by the new faculty startup funding by the Institute of Modern Physics, Chinese Academy of Sciences. This work is also supported by NSFC Grant No. 11705125.

References:

[1] LUZUM M, ROMATSCHKE P. Phys Rev C, 2008, **78**: 034915.

[2] SONG H, BASS S A, HEINZ U, *et al.* Phys Rev Lett, 2011, **106**: 192301.

[3] CHANG N, CAO S, CHEN B, *et al.* Phys Lett B, 2004, **595**: 165.

[4] RELAÑO A, GÓMEZ J M G, MOLINA R A, *et al.* Phys Rev Lett, 2002, **89**: 252301.

[5] AAMODT K, ABRAHANTES A, ADAMOVA D, *et al.* Phys Lett B, 2011, **696**: 30.

[6] LIN Z, KO C M, LI B, *et al.* Phys Rev C, 2005, **72**: 064901.

[7] MATSUI T, SATZ H. Phys Lett B, 1986, **178**: 416.

[8] EICHTEN E, GOTTFRIED K, KINOSHITA T, *et al.* Phys Rev D, 1978, **17**: 3090.

[9] EICHTEN E, GOTTFRIED K, KINOSHITA T, *et al.* Phys Rev D, 1980, **21**: 203.

[10] CREUTZ M, HORVÁTH I. Phys Rev D, 1994, **50**: 3.

[11] EICHTEN E, GOTTFRIED K, KINOSHITA T, *et al.* Phys Rev Lett, 1975, **34**: 6.

[12] KARSCH F, LAERMANN E. arXiv: hep-lat/0305025.

[13] BZDAK A, VLADIMIR S. Phys Rev B, 2012, **710**: 171.

[14] KARSCH F, PETRONZIO R. Z Phys C, 1988, **37**: 627.

[15] SATZ H. Journal of Physics G: Nuclear and Particle Physics, 2006, **32**: R25.

[16] KARSCH F, MEHR M T, SATZ H. Z. Phys. C, 1988, **37**: 617.

[17] GRECO V, VAN HEES H, RAAP R. AIP Conf Proc, 2012, **1442**: 117.

[18] DENG W, HUANG X. Phys Rev C, 2012, **85**: 044907.

[19] JACKSON J. Classical Electrodynamics[M]. 3rd ed. New Jersey: Wiley, 1998.

[20] HEYDE K. Basic Ideas and Concepts in Nuclear Physics: An Introduction Approach [M]. London: Bristol and Philadelphia, 1994.

[21] EARDEN I G B, BEAVIS D, BESLIU C, *et al* (BRAHMS Collaboration). Phys Rev Lett 2004, **93**: 102301.

[22] JORKEN J D B. Phys Rev D, 1983, **27**: 140.

[23] GUO X, SHI S, XU N. *et al.* Phys Rev B, 2015 **751**: 215.

[24] TUCHIN K. Adv High Energy Phys, 2013, **2013**: 490495.

[25] TOSHIAKI I. Phys Rev E, 1994, **49**: 4684.

强电场对夸克胶子等离子体中粲夸克偶素演化的影响

武表钢[1,2]，陈保义[3]，赵行波[1,2,†]

（1. 中国科学院近代物理研究所，兰州 730000;
2. 中国科学院大学核科学与技术学院，北京 100049;
3. 天津大学物理学系，天津 300350）

摘要： 在极端相对论性重离子碰撞中，高速运动的重离子会产生很强的电场。在碰撞的早期电场强度大小在$eE\sim m_\pi^2$的量级。在夸克胶子等离子体中，强电场将会对粲夸克偶素的演化产生巨大的影响。我们用含时薛定谔方程计算夸克胶子等离子体中由高速运动电荷所产生强电场对重夸克偶素演化的影响。此电场可以导致不同角动量态之间的跃迁。为了研究此效应，我们比较了有电场和无电场情况下J/ψ、ψ'以及χ_c的产额。计算结果表明，在碰撞早期电场会导致J/ψ解离；同时，χ_c也会由电场导致的J/ψ的跃迁而产生。

关键词： 粲夸克偶素；强电场；夸克胶子等离子体；薛定谔方程

收稿日期： 2019-03-25；　**修改日期：** 2019-05-05

基金项目： 国家自然科学基金资助项目(11705125)；中国科学院近代物理研究所青年千人计划基金

† **通信作者：** 赵行波，E-mail: xbzhao@impcas.ac.cn。